

Noise in β'' -alumina solid electrolytes: Theory and experiment

Carolyn M. Van Vliet

Department of Electrical and Computer Engineering, Florida International University, Miami, Florida 33199

James J. Brophy*

Department of Physics, University of Utah, Salt Lake City, Utah 84112

(Received 2 October 1991; revised manuscript received 21 August 1992)

Measurements of noise in β'' aluminas (Na, Pb, Ag, and Ca) showing diffusion noise spectra, with high-frequency asymptote $\omega^{-3/2}$, have been reported by Brophy and co-workers since 1985, both for ceramics and single crystals. Comparison with the standard formulas by Burgess, Lax and Mengert, and Van Vliet and Fassett, showed that the observed noise was 9 to 12 orders of magnitude too high. In the present paper this discrepancy is addressed and removed. A detailed analysis is presented based on the two-dimensional planar diffusive motion of ions and defects in the Beavers-Ross (BR) and anti-Beavers-Ross sites of the conduction plane. Coulomb interaction in the plane is shown to have little effect due to screening; however, the antiferroelectric coupling, which gives rise to superlattice ordering as observed by Collin *et al.*, causes correlated jumps within a coherence area, involving ambipolar motion of vacancy anti-BR sites, cation BR sites, and cation anti-BR sites. In addition, electrostatic induction via the spinel blocks couples the fluctuations in adjacent conduction planes. For Na- β'' and Pb- β'' single crystals quantitative agreement is obtained and the essential features of x-ray- and neutron-scattering data are confirmed.

I. INTRODUCTION: STRUCTURE AND CONDUCTIVITY OF THE β'' -ALUMINAS AND MOTIVATION OF PRESENT WORK

In the last decade and a half, physicists, chemists, and material science specialists have devoted much attention to solid electrolytes such as the β - and β'' -aluminas, either in single-crystal or ceramic form, because of their properties and applications ranging from batteries and electrochemical devices to ion-selective membranes. Some researchers use the name "superionic conductors" to indicate that these materials exhibit an unusually large ionic conductivity, which is associated with built-in stoichiometric defects. For a tutorial survey paper we refer to Bates, Wang, and Dudney.¹

Noise measurements on these materials, including Na-, Pb-, Ag-, and Ca- β'' -aluminas were reported from 1985–1990 by Brophy and co-workers.^{2–7} Two common features stand out in all the reported data. First, in the measured range from 3×10^{-3} Hz to 10^4 Hz the noise varies as $\omega^{-3/2}$, which is indicative for diffusion of rather slowly moving entities, such as ions or ion-defect conglomerates. Second, using known values of the diffusion constant and defect numbers, the noise appears to be a factor 10^9 – 10^{12} too high when compared with the elementary result for the high-frequency diffusion spectrum asymptote in an isotropic ν -dimensional domain ($\nu=1,2,3$), see Sec. II.

This is somewhat surprising since tracer diffusion (protons in Niobium) give noise which agrees quantitatively with the standard theory.⁸ It should be noted here that Brophy and co-workers used the simple one-dimensional (1D) result first derived by Burgess, but as later shown by Lax and Mengert,⁹ the high-frequency asymptote is the

same in all dimensions apart from a small geometry factor. Furthermore, the initial measurements, see in particular Ref. 2 for Na- β'' -alumina, indicated that the normalized noise $S_{\Delta I}/I_0^2$ did not exhibit the activation energy of $D^{1/2}$ [where $D=D_0 \exp(-\epsilon_d/kT)$, ϵ_d being the defect-motion activation energy, believed to be¹⁰ ≈ 0.31 eV for Na- β'' -alumina] but a much higher value. In retrospect this is attributed to contact problems and hygroscopic or other electrochemical effects. Later measurements, in which the effective density of diffusing entities was computed from the measured data and the theoretical result for diffusion noise in a finite embedded medium (see Sec. II A), led to values of n_{eff} which were only weakly temperature dependent when plotted versus $1000/T$, using the known activation energies, but with typical values of $n_{\text{eff}} \sim 10^{12}$ cm⁻³ for Na- β'' -alumina single crystals and $\sim 10^{11}$ cm⁻³ for Pb- β'' crystals. These later results are reproducible in time and from sample to sample and concern us here. Explicit data are given and summarized in Sec. III A. The conclusion can be made here, however, as in previously reported work, that the diffusing entities can be neither the totality of cations ($n_c \approx 10^{22}$ cm⁻³) nor the defect population ($n_d \approx 10^{21}$ cm⁻³). Therefore, *taking the measurements at face value*, the only options are that either a small fraction of the defects participates in the noise, or large correlations between diffusing entities occur. Having examined these options, we will argue in this paper that the latter possibility applies and fits in naturally with the well-known layered structure of these materials as well as with the x-ray crystallographic data for the single crystals.

The structure of β - and β'' -aluminas is well described in the article by Bates, Wang, and Dudney; see Ref. 1. In Fig. 1, we reproduce the structure of β -alumina as found

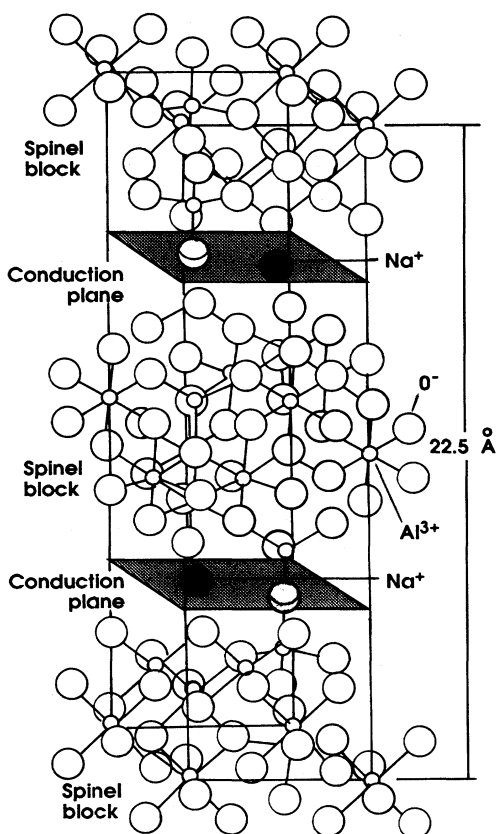


FIG. 1. Unit cell of β -alumina. After J. B. Bates, J. C. Wang, and N. J. Dudney (Ref. 1, Fig. 5). With permission.

in their paper. The gross structure of β' -alumina is the same, but the details of the conduction area are different, see Fig. 2. The sodium positive ions Na^+ are slightly above and below the geometrical plane between the spinel blocks. The latter are arranged along the c axis and separated by approximately 11.2 \AA , one-third the height of the unit cell. The width of a unit cell is $a_0 \times a_0$, with $a_0 = 5.62 \text{ \AA}$, see Fig. 2. The sodium ions have vacancies at specified places about one in four in a zig-zag path connecting nearest Na^+ neighbors, each sodium ion having three neighbors slightly below or above the plane considered. This leads to 17% vacancies in the two closely spaced (distance 0.4 \AA) sodium layers. Further, each sodium ion is coordinated by four oxygen ions, three in one layer and one in the opposite layer. The entire structure thus obtained is stoichiometric. E.g., for sodium β' -alumina the formula is $\text{Na}_{1.67} \text{Mg}_{0.67} \text{Al}_{10.33} \text{O}_{17}$; one easily sees that the positive charge is $1.67 + 2 \times 0.67 + 3 \times 10.33 = 34$, thus balancing the negative O^- charge. Thus, the vacancies are *globally* neutral, i.e., uncharged. *Locally*, however, a vacancy is a hole in the two-dimensional Na^+ sea, and carries therefore a negative charge. This is closely balanced by the Na^+ environment, in particular by the three nearest neighbors, each representing $\frac{1}{3}$ positive charge. In the elementary picture of Ref. 1, which will be amended later (see below and Sec.

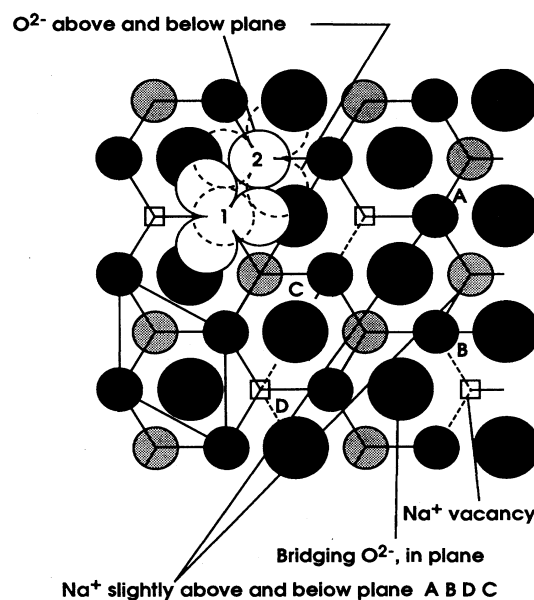


FIG. 2. Conduction plane of β' -alumina. After J. B. Bates, J. C. Wang, and N. J. Dudney [Ref. 1, Fig. 6(b)]. With permission.

II B 2) conduction takes place by hopping of a sodium ion into an adjacent vacancy, the latter being displaced in the opposite direction, in accordance with the negative charge we assigned to it. The two sodium layers, together with their coordinated oxygen ions, form a two-dimensional substructure in the unit cell, referred to as the conduction plane. No conduction takes place along the c axis since there are no vacancies in the spinel block, except for the thermodynamic number of Schottky defects, which is extremely small at room temperature, according to the mass-action law. The spinel blocks are therefore near-lossless dielectrics. *The two-dimensional conductivity is crucial for understanding the noise.* The conductivity tensor of a three-dimensional crystal has basically two components, σ_{\parallel} in the plane and σ_{\perp} along the c axis, with $\sigma_{\perp} \rightarrow 0$. In a ceramic the crystallites, of size $\sim 5 \times 10^{-4} \text{ cm}$, are randomly oriented. In that case an overall quasi-isotropic conductivity of $0.025 \Omega^{-1} \text{ cm}^{-1}$, comparable to the electronic conductivity of lightly doped semiconductors, is typical for these materials.

The considerations of this paper will mainly concern single crystals without crystallite boundaries. The conduction process is then described by standard 2D random walk considerations. Thus the diffusion constant is given by $D = \frac{1}{3} \nu a_0^2 e^{-\epsilon_d/kT}$, where $\frac{1}{3} a_0 \sqrt{3}$ is the spacing between sodium ion sites, ν is the escape frequency (involving phonon absorption), say $2.0 \times 10^{14} \text{ sec}^{-1}$, and ϵ_d the potential barrier to be overcome, close to 0.3 eV for $\text{Na}\beta'$ -alumina as we saw above. This results in a diffusivity of approximately $1.5 \times 10^{-6} \text{ cm}^2/\text{sec}$, as observed in this material. The mobility follows from Einstein's relation; thus at room temperature with $kT = 0.025 \text{ eV}$, $\mu \approx 6 \times 10^{-5} \text{ cm}^2/\text{V sec}$.

The above simple model neglects correlations of motion due to antiferroelectric coupling which gives rise

to superlattice ordering of the vacancies in the plane, as observed in x-ray-diffraction studies around 1980. These studies indicate the occurrence of a well-ordered structure, with a superlattice constant $a_0\sqrt{3}$, see Collin *et al.*¹¹⁻¹³ The coherence length ξ in the conduction planes at room temperature is about 70 Å for Na- β'' -, 35 Å for K- β'' -, and 200 Å for Pb- β'' -alumina. At higher temperatures the coherence length decreases, reaching a constant value of approximately 20 Å in Na- β'' -alumina as shown by patterns in the 500–1000 K range. In the cited studies it is indicated that the termination of coherence occurs due to an interchange of Beavers-Ross (BR) and anti-Beavers-Ross sites (these sites are the possible cation positions in opposite layers of the conduction plane, being separated only by a very small shift, see Fig. 2). A substructure of dimension ξ^2 will be called a *coherence area* (the term “domain” being less desirable, since there are no domain-wall barriers and overall continuity of structure is maintained, see Ref. 13, last part of Sec. IV). Within a coherence area the cations preferably occupy the BR sites while the vacancies are located at anti-BR sites in the opposite layer, as in the illustration of Fig. 2. Therefore, as to some extent discussed and implied by the models in the literature (see, e.g., Ref. 1, p. 50 under “superlattice ordering”), cation-vacancy jumps must be made in a correlated fashion within a coherence area in order to maintain the ordered structure; this is also born out by the observed high activation energy: 0.31 eV for Na- β'' , as compared to 0.02 eV expected for independent ion-vacancy hops. The cause of the quasi-long-range 2D order will be further discussed in Sec. II B 2. It will be shown there that the ordering has no effect on the “mean” or first-order moment of the fluctuating defect population, $\langle N_d \rangle = N_{d0}$. Thus, when computing the mean conductance one can treat the defects *as if* they moved independently; however, as noted above, the diffusion constant and the mobility, which are still related by the Einstein relation, involve a high energy-barrier activation energy due to the actual correlated motion, resulting in the low values of D and μ at room temperature given before. On the contrary, the second moment and variance of the defect population $\langle \Delta N_d^2 \rangle$ will be greatly affected by the correlated motion; a simple model will be considered later.

We now compare the two-dimensional description and alluded values for D and μ with the experimental results. Consider the Na- β'' -alumina single-crystal Na(1), described further in Sec. III A, which is in the form of a $0.5 \times 0.5 \times 0.05$ cm³ square platelet having the flat sides perpendicular to the c axis. One pair of diagonally opposed corner electrodes is used for carrying the current, while the other pair serve as probes for noise measurements, see Fig. 3. In diffusion noise measurements, the transverse contacts probe the conductance fluctuations in the subvolume area $abcd$. Nyquist noise measurements, however, involve the conductance of the rectangle spanned by $BbaD$ and $BcdD$. The conductance of a two-dimensional planar sheet is given by

$$G_1 = (e\mu n_{d0})(l/L), \quad (1.1)$$

where l is the width and L the length of the conducting

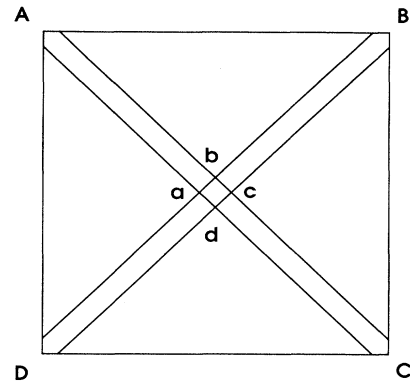


FIG. 3. Geometry of crystal platelets. Electrodes A and C carry the current. Electrodes B and D probe the conductance-fluctuation noise of area $abcd$ and measure the Nyquist noise.

path. For two cations per unit cell with a vacancy rate of 17%, the vacancy (defect) density per unit area is found to be $\langle n_d \rangle \equiv n_{d0} = 1.24 \times 10^{14}$ cm⁻². Clearly, see Fig. 3, the field lines from A to C and from B to D are curved, but suitable approximations are a width $l = 0.1$ cm and a length $L = 0.5\sqrt{2} = 0.7$ cm. With the above values of μ and n_{d0} Eq. (1.1) gives $G_1 = 1.70 \times 10^{-10}(\Omega)^{-1}$ for the conductance of one plane. The number of conduction planes will be denoted by K . For a thickness of 0.05 cm, there are $0.05 \div 11 \times 10^{-8} = 4.5 \times 10^5$ conduction planes in parallel, so that the resulting resistance is, writing $R_1 = 1/G_1 = 0.6 \times 10^{10}\Omega$,

$$R = R_1/K = R_1/4.5 \times 10^5 = 1.33 \times 10^4\Omega. \quad (1.2)$$

Nyquist noise measurements on crystal Na(1) yield $2.2 \times 10^4\Omega$ at a temperature of 294 K and $1.5 \times 10^4\Omega$ at 300 K. Clearly, the employed values are very reasonable in view of these results.

A further discussion of experimental results is given in Sec. III, after the presentation of various theories in Sec. II following below.

II. THEORETICAL MODELS

In Sec. II A we review the elementary theory of diffusion noise, while in Sec. II B we discuss correlations in the plane. In Sec. II C we consider the coupling of the planes, i.e., the possible correlations along the c axis.

A. The diffusion noise of a planar sheet, neglecting all correlations

The solution of the two-dimensional diffusion noise problem, based on an eigenfunction expansion of the Fourier-Laplace transform of the Green's function for the operator $\partial/\partial t + D\nabla^2 \equiv \partial/\partial t + \Lambda$ can be found in the article by Van Vliet and Fassett,¹⁴ henceforth denoted by VV-F. The solution occurs in the form of a double sum and gives little insight into the problem, unless numerical computations are performed, see Mehta.¹⁵ For a circle (or cylinder) a closed-form solution was given by Van Vliet and Chenette.¹⁶ The final result involves the Bessel functions of complex argument (ber, bei, ker, kei) in ac-

cordance with an earlier solution by Burgess.¹⁷ Fortunately, however, we are only interested in the high-frequency asymptote, which can be obtained rather simply.

It is generally assumed that this high-frequency asymptote of the noise spectrum for diffusion in an ν -dimensional geometry ($\nu=1,2,3,\dots$) goes as $\omega^{-3/2}$, as inferred from the article by Lax and Mengert.⁹ This, however, is not entirely true (nor stated without restrictions in Ref. 9). Conditional to the $\omega^{-3/2}$ behavior is that we consider the diffusion of particles in a subdomain V_s embedded in an infinite expanse $V \rightarrow \infty$. If the expanse V is finite, or even coincides with V_s , then the boundary conditions on the edge of V cause the final asymptote to be changed into ω^{-2} , though prior to this a $\omega^{-3/2}$ region may exist. Numerous examples are shown, in particular for V coinciding with V_s ("nonembedded problem"), in VV-F, the Van Vliet-Chenette paper, and in Harshad Mehta's thesis,¹⁵ 1981 (this study also refutes many features of the Voss-Clarke solution for heat diffusion, an analogous problem).¹⁸ Since Brophy observed a $\omega^{-3/2}$ spectrum in all cases, we clearly deal with an embedded diffusion problem. This is also born out by the geometry of Fig. 3. The transverse electrodes probe the noise from the subdomain $V_s = \text{area}(abcd)$, embedded in the crystal surface $V = \text{area}(ABCD)$. We denote by $N = \int_{V_s} n_d dA$ the total number of defects involved in diffusion and we seek the spectrum of ΔN associated with transport through the "fictitious boundaries" (term of Lax) with the shell $V - V_s$. The high-frequency (hf) asymptote in any geometry is most easily obtained from the generalized Richardson's formula,¹⁹ see also VV-F, Eq. 272(a). The result given there is correct for self-adjoint transport operators Λ . A more general result, using a biorthogonal eigenfunction expansion of the Green's function was derived in a survey paper by Van Vliet and Mehta²⁰ (denoted as VV-M). The complete result is in Eq. (2.33) of that paper:

$$S_{\Delta N}(\omega) = \frac{4\langle \Delta N^2 \rangle}{V_s} \text{Re} \int_{V_s} \int_{V_s} d^{\nu} r d^{\nu} r' \sum_k \frac{\phi_k(\mathbf{r}) \psi_k^*(\mathbf{r}')}{\lambda_k + i\omega}, \quad (2.1)$$

where $\phi_k(\mathbf{r})$ are the eigenfunctions (EF) of Λ , ψ_k of Λ^\dagger , while λ_k, λ_k^* are the complex eigenvalues (EV) of these operators, respectively. For the diffusion problem $e^{i\mathbf{k}\cdot\mathbf{r}}/V_s^{1/2}$ are the EF of the self-adjoint operator $D\nabla^2$ in any dimensionality ν , the EV being $-Dk^2$. Further, the sum in (2.1) is replaced by $\sum_k \rightarrow [V_s/(2\pi)^\nu] \int d^\nu k$. We then obtain, see VV-M, Eq. (2.55),

$$S_{\Delta N}(\omega) = \frac{4\langle \Delta N^2 \rangle}{V_s (2\pi)^\nu} \int \frac{d^\nu k D k^2}{D^2 k^4 + \omega^2} \left| \int_{V_s} d^{\nu} r e^{i\mathbf{k}\cdot\mathbf{r}} \right|^2. \quad (2.2)$$

Because of the radial symmetry of (2.2) in \mathbf{k} space, the hf asymptote is most easily found by considering V_s to be a circle of diameter l , rather than a square. The error so obtained is of order $4/\pi$. For the $\|\cdot\|^2$ factor in (2.2) we have,

$$\begin{aligned} \int_{V_s} d^2 r e^{i\mathbf{k}\cdot\mathbf{r}} &= \int_0^{l/2} r dr \int_0^{2\pi} d\varphi e^{i\mathbf{k}r \cos\varphi} d\varphi \\ &= 2\pi \int_0^{l/2} r dr J_0(kr) \\ &= 2\pi(l/2k) J_1(kl/2), \end{aligned} \quad (2.3)$$

where J_0 and J_1 are Bessel functions of the first kind. Further,²¹

$$|J_1(kl/2)|^2 \sim \frac{4}{\pi kl} \cos^2 \left[kl/2 - \frac{3}{4}\pi \right] = \frac{2}{\pi kl}. \quad (2.4)$$

We are left with the integral²²

$$\int_0^\infty \frac{dk}{D^2 k^4 + \omega^2} = \frac{\pi}{D^2} \left[\frac{D}{2\omega} \right]^{3/2}. \quad (2.5)$$

The final result is, setting $\langle \Delta N^2 \rangle = N_0$ for Poissonian noise,

$$S_{\Delta N}(\omega \text{ large}) = \frac{16N_0}{Dl} \left[\frac{D}{2\omega} \right]^{3/2}. \quad (2.6)$$

Now let I_1 be the current flow due to one conduction plane and let $S_{I_1}(\omega)$ be the corresponding spectrum. The normalized noise goes as $1/N_0$ as it should be,

$$\frac{S_{I_1}(\omega)}{I_{10}^2} = \frac{S_{\Delta N}(\omega)}{N_0^2} = \frac{16}{DlN_0} \left[\frac{D}{2\omega} \right]^{3/2}. \quad (2.7)$$

Let the total current to probe the conductivity fluctuations be $I = \sum_{i=1}^K I_{1,i} = KI_1$, where K is the number of conducting layers in parallel. For the noise we have

$$S_I(\omega) = \sum_i S_{I_{1,i}I_{1,i}} + \sum'_{i,j} S_{I_{1,i}I_{1,j}}, \quad (\sum' \text{ means } i \neq j), \quad (2.8)$$

where $S_{I_{1,i}I_{1,j}} \propto S_{\Delta N_i, \Delta N_j}$. The first sum is KS_{I_1} and if there is no correlation between conduction planes, the second sum is zero. Then we find, restoring for generality and later reference the variance in the numerator,

$$\frac{S_I(\omega)}{I_0^2} = \frac{1}{K} \frac{S_{I_1}(\omega)}{I_{10}^2} = \frac{16\langle \Delta N^2 \rangle}{DKlN_0^2} \left[\frac{D}{2\omega} \right]^{3/2}. \quad (2.9)$$

On the other hand, if the fluctuations in adjacent layers are fully correlated, then the second sum in (2.8) equals $K(K-1)S_{I_1}$, so that $S_I(\omega) = K^2 S_{I_1}(\omega)$. In that case the total noise is

$$\frac{S_I(\omega)}{I_0^2} = \frac{S_{I_1}(\omega)}{I_{10}^2} = \frac{16\langle \Delta N^2 \rangle}{DlN_0^2} \left[\frac{D}{2\omega} \right]^{3/2}, \quad (2.10)$$

i.e., the observed normalized noise is the same as the normalized current or number fluctuations [Eq. (2.7)] for a single conduction plane.

B. Electrostatic effects in the conduction plane

1. Effects of the Coulomb field; the density-density correlation function

The effect of the Coulomb field arising from the charged defects mentioned in several already quoted pa-

pers is, in our opinion, greatly misunderstood. In particular, the Coulomb field does not produce long-range correlations, nor does it give rise to a large modulation factor for the noise. In this subsection we briefly indicate that the Coulomb field is very strongly screened in both the Debye-Hückel and plasmon-frequency model, while the density-density correlations contribute at most a modulation factor of 2 to the magnitude of the noise. The Debye-Hückel theory for screening of the Coulomb potential in a globally neutral plasma has been with us²³ since 1923. They found from a simple argument that the screening of one charge by a "sea" of other charges screens the Coulomb potential, so as to give it a finite range. The sign of the background charges is immaterial since the screening length contains q^2 , with $q = \pm Ze$. Thus a positive charge can be screened by a sea of negative charge, as well as by other positive charges. From the screened Coulomb field and associated free energy the density-density correlation function follows. A more fundamental computation, based on the partition function for the Coulomb gas, due to Bogoliubov (1946) is found in Landau and Lifshitz.²⁴ Finally, a non-equilibrium approach, based on the master equation and the Λ theorem²⁵ was given by Van Vliet²⁶ in 1971. This method is of interest here since it is equivalent to the idea of a correlated random walk due to "potential feedback," as suggested by Forgacs and Kiss.²⁷ Thus, it takes into account that a jump by one charged particle changes the potential barrier through Poisson's equation; this in turn affects the next carrier, etc. . . . The three-dimensional (3D) case is found in Ref. 26. The density-density correlation function $\langle \Delta n(\mathbf{r}) \Delta n(\mathbf{r}') \rangle$ consists of a δ -function part $\delta(\mathbf{r}-\mathbf{r}')$ ("dimensional singularity"), and a part involving the familiar Helmholtz function $e^{-\kappa|\mathbf{r}-\mathbf{r}'|}/|\mathbf{r}-\mathbf{r}'|$. The extension to the 2D case is straightforward. We briefly indicate the procedure and the results.

Let 2δ be the thickness of the conduction "plane." The density (per unit volume) of a species will be denoted by \hat{n}^i and the charge by q^i . The plasma containing $i = 1 \dots s$ species is assumed to be neutral. The continuity equation for each species reads

$$\frac{\partial \hat{n}^i}{\partial t} + \frac{1}{q^i} \text{div} \mathbf{J}^i = 0, \quad (2.11)$$

while the current satisfies the stochastic equation,

$$\mathbf{J}^i = q^i \hat{n}^i \underline{\mu}^i \cdot \mathbf{E} - q^i \underline{D}^i \cdot \text{grad} \hat{n}^i + q^i \hat{\eta}^i(\mathbf{r}, t), \quad (2.12)$$

$\hat{\eta}(\mathbf{r}, t)$ being the Langevin source responsible for diffusion (as well as for Nyquist noise if $\mathbf{E} = 0$). We write $\hat{n}^i = \hat{n}_0^i + \Delta \hat{n}^i$, $\mathbf{J}^i = \mathbf{J}_0^i + \Delta \mathbf{J}^i$, $\mathbf{E} = \mathbf{E}_0 + \Delta \mathbf{E} \approx \Delta \mathbf{E}$, which yields, neglecting terms $O(\Delta^2)$ and setting $\nabla \hat{n}_0^i \approx 0$ for a globally homogeneous system,

$$\partial \Delta \hat{n}^i / \partial t + \hat{n}_0^i \underline{\mu}^i : \nabla (\Delta \mathbf{E}) - \underline{D}^i : \nabla \nabla (\Delta \hat{n}^i) = -\nabla \cdot \hat{\eta}^i(\mathbf{r}, t). \quad (2.13)$$

In accordance with the preceding model we assume that the tensors \underline{D} and $\underline{\mu}$ mainly have a component D_{\parallel} and μ_{\parallel} in the plane, the perpendicular components D_{\perp} and μ_{\perp} being near zero. Further, for radial planar symmetry Poisson's equation reads

$$\text{div}_r(\Delta \mathbf{E})_r + \text{div}_z(\Delta \mathbf{E})_z = \sum_{j=1}^s q^j \Delta \hat{n}^j / \epsilon \epsilon_0. \quad (2.14)$$

Integrating along the z axis perpendicular to the conduction plane over the layer 2δ , and denoting by n^j , densities in the plane (per unit area) we find

$$2\delta \text{div}_r(\Delta \mathbf{E})_r + \Delta E_z|_{-\delta}^{\delta} = \sum_{j=1}^s q^j \Delta n^j / \epsilon \epsilon_0. \quad (2.15)$$

Since the right-hand side (rhs) is a double layer of opposite charges (*dipole layer*), the field along the z direction (c axis) jumps. We come back to this in Sec. II C.

We now substitute (2.15) into (2.13) and obtain the stochastic transport equations in matrix form,

$$[(\partial/\partial t)\underline{I} + \underline{\Lambda}][\Delta n] = -[\nabla \cdot \underline{\eta}], \quad (2.16)$$

where \underline{I} is the unit matrix; $\underline{\Lambda}$ has the components

$$\Lambda_r^{ij} = -\delta^{ij} D_{\parallel}^i \nabla_r^2 + q^i q^j n_0^i D_{\parallel}^j / 2\delta k T \epsilon \epsilon_0, \quad (2.17)$$

where we used the Einstein relation. The density-density correlation function $\langle \Delta n^i(\mathbf{r}) \Delta n^j(\mathbf{r}') \rangle \equiv \Gamma^{ij}(\mathbf{r}, \mathbf{r}')$ satisfies the Lambda theorem (Ref. 25, see also Wang and Uhlenbeck²⁸):

$$\sum_k [\Lambda_r^{ik} \Gamma^{kj}(\mathbf{r}, \mathbf{r}') + \Lambda_r^{jk} \Gamma^{ik}(\mathbf{r}, \mathbf{r}')] = \frac{1}{2} S^{ij}(\mathbf{r}, \mathbf{r}'), \quad (2.18)$$

where Λ_r operates on the coordinate r and Λ_r on r' ; S^{ij} is the white spectrum of the Langevin source function,

$$S^{ij}(\mathbf{r}, \mathbf{r}') = 4D_{\parallel}^i \nabla_r \cdot \nabla_{r'} [n_0^i(\mathbf{r}) \delta^{(2)}(\mathbf{r}-\mathbf{r}')] \delta^{ij}, \quad (2.19)$$

where $\delta^{(2)}$ is a δ function in the plane. We neglect local inhomogeneity, $\nabla n_0^i(\mathbf{r}) \approx 0$ and make the ansatz

$$\Gamma^{ij}(\mathbf{r}, \mathbf{r}') = n_0^i \delta^{(2)}(\mathbf{r}-\mathbf{r}') \delta^{ij} + n_0^i n_0^j q^i q^j \omega(\mathbf{r}, \mathbf{r}'). \quad (2.20)$$

The set of equations (2.18) is then identically satisfied by the Helmholtz equation

$$\nabla_r^2 \omega - \kappa^2 \omega = \nabla_r^2 \omega - \kappa^2 \omega = (\kappa^2 / \sum_k n_0^k (q^k)^2) \delta^{(2)}(\mathbf{r}-\mathbf{r}'), \quad (2.21)$$

where

$$\kappa^2 = \sum_k n_0^k (q^k)^2 / 2\delta k T \epsilon \epsilon_0 \quad (2.21a)$$

is the squared reciprocal Debye length. In cylindrical coordinates with $R = (\mathbf{r}-\mathbf{r}')$,

$$\frac{d^2 \omega}{dR^2} + \frac{1}{R} \frac{d\omega}{dR} + \kappa^2 \omega(R) = C \delta^{(2)}(\mathbf{r}-\mathbf{r}'), \quad (2.22)$$

subject to the boundary conditions $\omega(R \rightarrow 0) = (C/2\pi) \ln(\kappa R/2) \rightarrow -\infty$ and $\omega(R \text{ large}) \sim 0$. Clearly, then, $\omega(R) = 4CY_0(R)$ where Y_0 is the Neumann function. For a graph, see Ref. 21, p. 359. The damping is now *oscillatory* in κR with the second zero crossing occurring near $\kappa R = 4$. In the next section we will see that "a jump" basically includes one vacancy (charge $-e$) and two neighboring cations (each representing a charge $+e/2$). We thus find from (2.20)–(2.22), noticing that equal densities of the three species are involved,

$$\langle \Delta n_v(\mathbf{r}) \Delta n_v(\mathbf{r}') \rangle = n_{v0} \delta^{(2)}(\mathbf{r} - \mathbf{r}') + \left(\frac{8}{3}\right) n_{v0} \kappa^2 Y_0(\kappa R). \quad (2.23)$$

For strong screening, $\kappa R \rightarrow \infty$, we have $\kappa^2 Y_0(\kappa R) \rightarrow -(\frac{1}{4})\delta^{(2)}(\mathbf{r} - \mathbf{r}')$. Then for the density-density correlation function, $\Gamma(\mathbf{r}, \mathbf{r}') \rightarrow (n_{v0}/3)\delta^{(2)}(\mathbf{r} - \mathbf{r}')$. The factor $\frac{1}{3}$ represents the deviation from Poissonian statistics associated with a cubic generation-recombination law for the constituting defect species, as can be seen from the master equation for the jump process, or more directly from Burgess's g - r theorem.²⁹

For moderate screening the full results (2.23) must be used. We still mention that the article VV-M gives the spectrum when the density-density correlation function is not a δ function, *op.cit.* Eq. (2.19). Instead of Richardson's formula (2.2) we have more generally for correlated diffusion

$$S_{\Delta N}(\omega) = \frac{4}{(2\pi)^{\nu}} \text{Re} \int_{-\infty}^{\infty} d^{\nu}k \int_V d^{\nu}r'' \int_{V_s} d^{\nu}r \times \int_{V_s} d^{\nu}r' \Gamma(\mathbf{r}'', \mathbf{r}') \frac{e^{i\mathbf{k} \cdot (\mathbf{r} - \mathbf{r}')}}{Dk^2 + i\omega}. \quad (2.24)$$

For two dimensions, the substitution of (2.23) leads again to an exercise in Bessel function integrals. For 1D and 3D cases we have evaluated (2.24) explicitly and shown that its magnitude exceeds that of Eq. (2.2) by at most a factor of 2. Thus, large modulation factors cannot result from Coulomb interaction of free mobile charges. More disappointing is that for the case at hand the screening is strong. We saw above $n_{v0} \approx 10^{14} \text{ cm}^{-2}$. With $\delta = 0.4 \text{ \AA}$ and $\epsilon\epsilon_0 \approx 10^{-10}$, we find at 300 K, $\kappa^{-1} \approx 0.5 \text{ \AA}$. Such a small screening length implies that the continuum aspects of Debye-Hückel theory are not really valid. In such a case it is more realistic to employ a plasmon model, in which case one considers the quantized collective vibrations, associated with the polarization field $q\delta r/\epsilon\epsilon_0$ of a displaced charge. The equation of motion, $M\ddot{x} + q^2\hat{n}x/\epsilon\epsilon_0 = 0$, where $x = \delta r$ and M the ion mass, gives the plasmon frequency $\omega_p = (\hat{n}q^2/M\epsilon\epsilon_0)^{1/2}$. It is easily shown that this leads to an inverse screening length $\kappa \sim (\omega_p/v_d)$, v_d being the velocity acquired in the displacement (jump). One then finds that this leads to a similar expression for κ^2 , with kT replaced by the activation energy ϵ_d . The change in screening length (2.0 \AA) is insignificant.

2. Electric dipole-dipole interaction

We have seen above that the dipole field created by the displacement of the plasma charges does not cause a long-range order; on the contrary, the Coulomb field in the plane is strongly screened. Therefore, the correlation effects as noted in the supercell arrangement of the defects can only be caused by permanent dipole-dipole interaction in the slab which constitutes the conduction plane. A many-body quantum description of such effects is not available for these crystals at present. X-ray studies have confirmed that an antiferroelectric order (polarization $\uparrow\downarrow$) exists due to slight displacements of the cat-

ions and defects in the two layers of the conduction plane parallel to the c axis.¹³ A classical computation of the planar ordering energy ($\propto l^2$) and of the energy associated with a line of BR-anti-BR shifts in the plane ($\propto l$) gives by a Helmholtz free-energy minimization procedure the coherence length $l_{\min} = \zeta$ [(Ref. 13, Fig. 8 and Eq. (3.6)]. For Na- β'' this yields at room temperature $\zeta \approx 70 \text{ \AA}$. Moreover, the model explains that the BR sites and anti-BR sites are not equivalent in energy, see Fig. 4. Therefore, the anti-BR sites are preferably empty and a single hop, cation (BR site) \rightleftharpoons vacancy (anti-BR site), is highly improbable. Rather, the cations stay mainly at the BR sites. Contrary to the statement that in the new picture "there is no vacancy-motion process" (Ref. 13, Sec. III C), we still believe that vacancy motion is the catalyst. With reference to Figs. 2 and 4, noting that a vacancy will stay on an anti-BR site, its motion involves a twofold hop: anti-BR \rightarrow BR \rightarrow anti-BR. The first move involves exchange with a cation occupying a BR site and the subsequent move exchange with a cation occupying an anti-BR site. Within the coherence area, the other vacancies and their environment make identical jumps, so that the supercell structure is maintained. This more complex process involves three species in the defect motion.

Though sophisticated theories on correlated random walk are known,³⁰ a simple argument suffices here. Let N'_d be the number of defects in a coherence area and let P be the number of vacancy anti-BR sites, each site having an occupancy n_α , being zero or one with probability $p(\alpha)$. Clearly $N'_d = \sum_{\alpha=1}^P n_\alpha$. If the sites changed independently, the generating function would have the familiar form $\langle z^{N'_d} \rangle = \prod_{\alpha} \langle z^{n_\alpha} \rangle = \langle z^{n_\alpha} \rangle^P$. For the present case we have however,

$$\Phi(z) \equiv \langle z^{N'_d} \rangle = \sum_{n_1 \cdots n_p} W(n_1 \cdots n_p) z^{\sum_{\alpha=1}^P n_\alpha}, \quad (2.25)$$

where now due to correlation,

$$W(n_1 \cdots n_p) = p(\alpha) \delta_{n_1, n_\alpha} \cdots \delta_{n_p, n_\alpha}. \quad (2.26)$$

This yields,

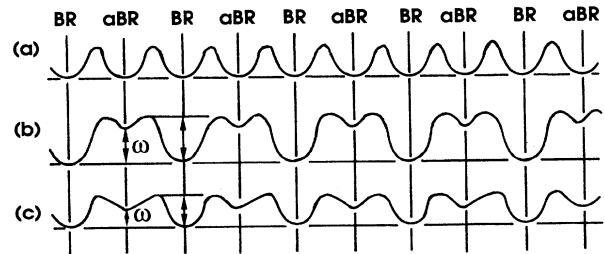


FIG. 4. Potential profile of BR and anti-BR sites in the two layers constituting the conduction plane. After G. Collin, J. P. Boilot, and R. Comes (Ref. 14, Fig. 11). With permission. (a) Conventional model in which the BR sites and anti-BR sites are equivalent. (b) Realistic situation in which in-plane correlations lower the energy of one site with respect to the other. (c) Same for higher temperature.

$$\Phi(z) = \sum_{n_\alpha} p(\alpha) z^{P n_\alpha} = \langle z^{P n_\alpha} \rangle. \quad (2.27)$$

The factorial moments follow from differentiation,

$$\Phi'(z)|_{z=1} = \langle N'_d \rangle = P \langle n_\alpha \rangle, \quad (2.28a)$$

$$\Phi''(z)|_{z=1} = \langle N'_d(N'_d - 1) \rangle = P^2 \langle n_\alpha^2 \rangle - P \langle n_\alpha \rangle. \quad (2.28b)$$

The first moment is not affected, i.e., the defects move *as if* they were independent. For the second moment and variance we find, however,

$$\begin{aligned} \langle \Delta N_d'^2 \rangle &= \langle N'_d(N'_d - 1) \rangle - \langle N'_d \rangle (\langle N'_d \rangle - 1) \\ &= P^2 [\langle n_\alpha^2 \rangle - \langle n_\alpha \rangle^2] \\ &= (P^2/3) \langle n_\alpha \rangle = (P/3) N_{d0}'. \end{aligned} \quad (2.29)$$

For the variance in an area V_s with occupancy N_d , we add the various coherence areas incoherently. Thus also,

$$\langle \Delta N_d^2 \rangle = (P/3) N_{d0}, \quad P = \xi^2 / 3a_0^2, \quad (2.30)$$

where the value of P is based on the area of the superlattice unit cell. For β -alumina the same result obtains since the "interstitialcy mechanism" also involves three species.¹

We should now once more consider the effect of the correlations on the spectrum. The density-density correlation function can in principle be found from the Helmholtz free energy. The main contribution is expected to be of the form

$$\begin{aligned} \langle \Delta n_d(\mathbf{r}) \Delta n_d(\mathbf{r}') \rangle &= P n_{d0} \delta^{(2)}(\mathbf{r} - \mathbf{r}') \\ &+ \frac{8}{3} P n_{d0} \xi^{-2} Y_0(|\mathbf{r} - \mathbf{r}'|/\xi). \end{aligned} \quad (2.31)$$

While these are significant correlations, when an integration over an area V_s of radius $R \gg \xi$ is performed, as required by (2.24), the latter term still contributes approximately $-\frac{2}{3}$ of the first term. Thus the old result for the high-frequency asymptote of Sec. II A still applies, by and large, providing the variance (2.30) is employed.

C. Correlation between the conduction planes

The last point to explain is that the various conduction planes cannot be treated as a set of uncorrelated conductors in parallel. In effect, it is perfectly legitimate and sufficient to consider the diffusion and noise of just one plane, in order to obtain the terminal results. If, nevertheless, we focus our attention on the entire array of conduction planes perpendicular to the c axis, we must realize that the strongly insulating behavior of the spinel blocks causes correlations of the fluctuations along the c axis, strong enough to fully couple adjacent planes, which are a mere 11.2Å apart. This is basically a manifestation of electrostatic induction.³¹ We have seen that the defects in the conduction plane comprise a dipole layer, see Eq. (2.15). Thus the field lines emanate from the positive charges in one plane and terminate on the negative charges in the adjacent plane. Therefore the charges in different planes line up. Actually we suggest that the full mosaic of the coherence areas in the various planes is re-

peated, with reversal in sign of the electric field along the c axis occurring at boundary lines of BR-anti-BR shifts in the planes. This would also explain that the x-ray patterns of a thin 3D crystal show a collective 2D ordering. If, on the contrary, as stated in some papers, the spinel blocks decouple the set of conduction planes, the 2D coherence pattern would be washed out.

The final problem is to obtain an estimate for the extinction length z_c for this coupling. In Sec. II B 1, we neglected D_\perp and μ_\perp . For the sake of argument, let us assume the values $D_\perp = 10^{-10} \text{ cm}^2$ and $\mu_\perp = 4 \times 10^{-9} \text{ cm}^2/\text{V sec}$; this corresponds to a jump potential of $\epsilon_d \approx 0.6 \text{ eV}$. Whereas cation-vacancy pairs, if spontaneously formed, depend on half the formation energy, the number of Schottky defects, i.e., vacancies occurring by themselves in the bulk, goes as $\exp(-W_s/kT)$. Generally we have, see Mott and Gurney,³²

$$n_{vS}/N = \gamma B e^{-W_s/kT}, \quad (2.32)$$

where $B = e^{4.8} \sim 100$ and $\gamma \sim 64$. The energy W_s to dislodge a cation in a spinel is of order 1 eV. With $N \sim 10^{22}/\text{cm}^3$ this yields $n_{vS} \approx 2.5 \times 10^8 \text{ cm}^{-3}$. For the correlation length we now obtain

$$z_c = (\epsilon_d \epsilon_0 / e^2 n_{vS})^{1/2} \approx 1.2 \times 10^{-3} \text{ m},$$

which is to be compared with the thickness of the crystal, $d = 5 \times 10^{-4} \text{ m}$. Whatever the precise values, it is very likely that there is very long-range correlation of the fluctuations $\langle \Delta n_v(z) \Delta n_v(z') \rangle$ along the c axis.

In conclusion, to describe the noise we can employ the basic results of Sec. 2 which for full correlation between the planes leads to Eq. (2.10). A modification for Coulomb interaction and plasma effects in the plane is unnecessary because of the strong screening. On the other hand, correlated motion due to antiferroelectric dipole-dipole interaction within a coherence area constitutes a modulation factor P , leading to a variance given by Eq. (2.30). This yields for the magnitude of the noise

$$\frac{S_I(\omega)}{I_0^2} = \frac{16P}{3D \ln N_{d0}} \left[\frac{D}{2\omega} \right]^{3/2}, \quad P = \frac{\xi^2}{3a_0^2}. \quad (2.33)$$

Compared to the result of Eq. (2.9), with Poissonian variance, reflecting the ideas in the earlier papers,²⁻⁷ this indicates an overall correlation factor of $PK/3$, which is of order 10^7 , see above Eq. (1.2) for a typical value of K and see the next section (Sec. III A) for P .

III. EXPERIMENTAL RESULTS

A. Typical experimental data

The experimental data for the β' -aluminas are found in Refs. 2-7 (we note incidentally that Ref. 5 also gives data for Na- β -alumina single crystals). Details of the experimental techniques used to measure conductivity fluctuations in the β' -aluminas have been described previously. Briefly, the corners of square single-crystal platelets or ceramic samples, approximately 0.5 to 1.0 cm on a side and 0.03 to 0.10 cm thick, are sealed into the sides of plastic test tubes containing solutions having the ionic

species of the mobile ion in the sample. As noted in connection with Fig. 3, one pair of diagonally opposed corner electrodes is used for current contacts and the other pair to measure transverse noise voltages with a PAR 113 preamplifier and a digital FFT analyzer. Suitable electrode solutions (e.g., 0.5-M NaI in propylene carbonate for Na- β'' -alumina) yield low-noise contacts after aging for several hours.^{3,6}

Typical noise spectra for a Na- β'' -alumina ceramic are shown in Fig. 5. The current noise spectra have the $-\frac{3}{2}$ slope characteristic of diffusion noise and the noise magnitude is proportional to the square of the current. In the absence of current, Nyquist noise corresponding to the sample resistance is visible above amplifier noise at frequencies greater than about 100 Hz. Similar features are seen in results for single-crystal Pb- β'' -alumina, Fig. 6, and for single-crystal Ag- β'' alumina, Fig. 7. Transverse and longitudinal noise levels are close to equal in the case of the Pb- β'' -alumina crystal, Fig. 6, indicative of minimal contact current noise. In the longitudinal arrangement, it is not clear, however, what part of the crystal makes up the "embedded area" so only the transverse noise level data are employed.

Room-temperature parameters of several single-crystal samples are summarized in Table I. Values for the conductivity are calculated from the sample dimensions and resistance as determined from the Nyquist noise. The agreement with literature values is good, given the rather unfavorable geometry of these square samples for conductivity studies and the known sensitivity of the conductivity to crystal growth conditions. Corresponding values for diffusion constants calculated from the conductivities and the Einstein relation are also in good agreement with the literature. For example, the measured room-

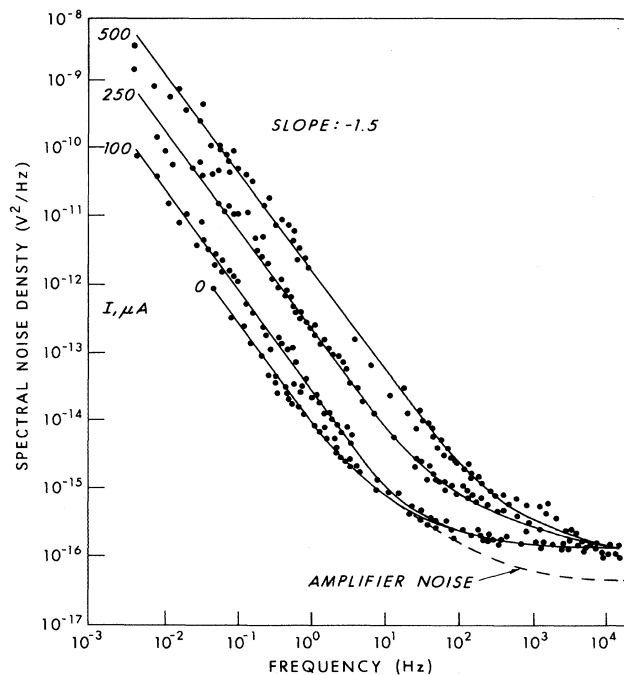


FIG. 5. Diffusion noise spectra of a Na- β'' -alumina ceramic at room temperature.

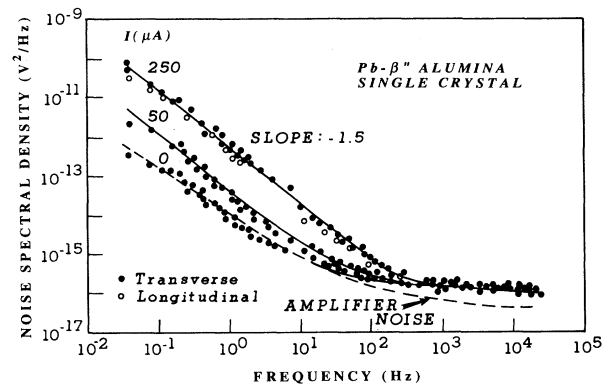


FIG. 6. Transverse and longitudinal diffusion noise spectra of a Pb- β'' -alumina single crystal.

temperature diffusion constant for crystal Na(1) is 1.5×10^{-6} cm²/sec. The activation energies for the diffusion constants are found from the variation of Nyquist noise with temperature over the limited range (260–340 K) around room temperature permitted by the liquid electrodes.

It is experimentally convenient to measure the transverse noise voltage and longitudinal dc current and derive values of $S_I(\omega)/I^2$ by dividing by the square of the resistance between the terminals, as determined from Nyquist noise, in accordance with Thévenin's theorem. [Since the resistance relates to the full sample length, the derived values of $S_I(\omega)/I^2$ may be viewed in the nature of a linear noise density.] Clearly, S_I/I^2 , so determined, relates to relative conductivity and defect number fluctuations of the embedded area, $S_{\Delta\sigma}/\sigma_0^2 = S_{\Delta N}/N_0^2$, the latter ratio being the noise computed in the previous sections.

The temperature variation of the measured diffusion noise, shown in Fig. 8 and normalized in accordance with Eq. (2.33), using literature values of ϵ_d , still exhibits a weak temperature dependence which fits the form

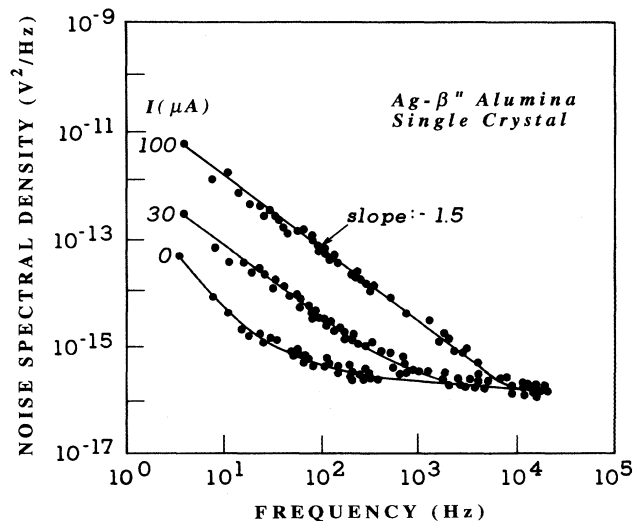


FIG. 7. Diffusion noise spectra of an Ag- β'' -alumina single crystal.

TABLE I. Room-temperature parameters of β'' -alumina single crystals.

Mobile ion	σ (Ω cm) $^{-1}$		ϵ_d (eV)		$\Delta\epsilon_c$ (eV)	$S_I(2\pi 10)/I^2$ (sec)	
	Measured	Literature	Measured	Literature	Measured	Measured	Calculated
Na(1)	0.01	0.014	0.49	0.31	0.035	1.9×10^{-15}	1.6×10^{-15}
Na(2)	0.01	0.014	0.29	0.31	0.049	1.6×10^{-15}	1.6×10^{-15}
Pb	0.008	0.005	0.32	0.25	0.033	2.7×10^{-14}	2.0×10^{-14}
Ag	0.006	0.004	0.22	0.19	0.090	5.1×10^{-13}	3.3×10^{-17}

$$P(T) = P(\infty) e^{2\Delta\epsilon_c/kT}, \quad (3.1)$$

where $\Delta\epsilon_c$ is the coherence energy pertaining to $\zeta(T)$. In this interpretation, based on the model in Secs. II B 2 and II C, the coherence length decreases with temperature, reaching the limiting value $P(\infty)$ at high temperature. This is in agreement with x-ray data (see Ref. 11, Fig. 5) and with theory (Ref. 13, Sec. III B 2) since the antiferroelectric order weakens when the temperature increases. The data of Ref. 11 plotted on a semilog scale yield a slope of $\Delta\epsilon_c \approx 0.1 \ln(1.4) = 0.034$ eV in good agreement with the values in Table I, except, perhaps, in the case of Ag- β'' -alumina.

B. Noise magnitude

The predicted magnitude of the diffusion noise for the Na-crystal at a frequency of 10 Hz follows directly from Eq. (4.2), using the 70\AA correlation length found from x-ray analysis,

$$P = \frac{\zeta^2}{3a_0^2} = \frac{(70)^2}{3(5.62)^2} = 52, \quad (3.2)$$

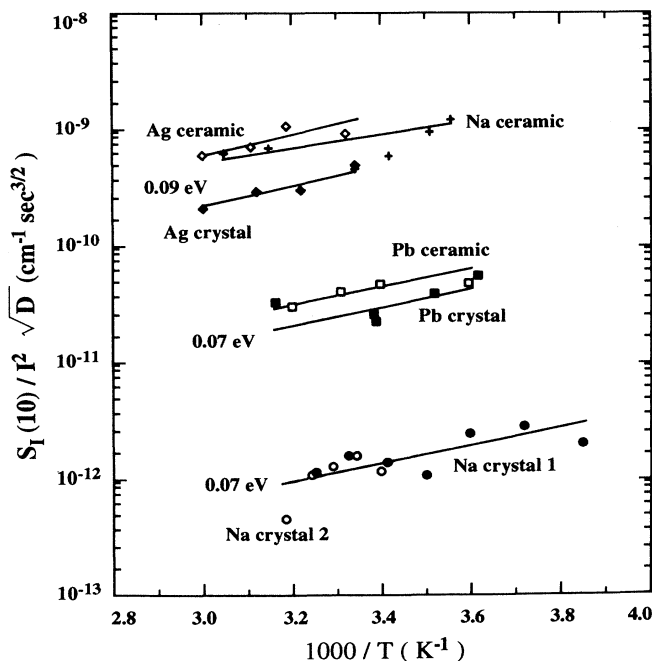


FIG. 8. Normalized diffusion noise at a frequency of 10 Hz as a function of reciprocal temperature for Na-, Pb-, and Ag- β'' -alumina single crystals and ceramics.

and the total number of defects in the 0.1×0.1 cm 2 imbedded region,

$$N_{d0} = 0.1 \times 0.1 \times 1.24 \times 10^{14} = 1.24 \times 10^{12}. \quad (3.3)$$

The result, given in the last column of Table I, is in remarkably good agreement with the experimental value. For Pb- β'' -alumina the vacancy rate is somewhat higher, presumably $\approx 22\%$ and the x-ray coherence length in this case is 200\AA , which gives $P=422$; again the prediction of Eq. (2.33) corresponds quite well to the measured data.

This agreement is not found for Ag- β'' -alumina, using the literature coherence length of 10\AA . There is, however, some uncertainty in this value and the x-ray data appear to indicate some three-dimensional ordering. Also, the value of $\Delta\epsilon_c$ found from the noise measurements is significantly greater than those for Na- and Pb- β'' -alumina. On the basis of the model and the noise measurements, a coherence length of 1000\AA is predicted, which seems rather unlikely. These observations suggest that Ag- β'' -alumina may not fit the present noise model.

Ceramic samples are consistently noisier than single crystals, as shown in Fig. 8. Although the ceramics appear to be quasi-isotropic, the conduction remains two dimensional, tracing zig-zag paths through the sample since the crystallite grains do not match. Typically, there are 2×10^3 crystallites/cm of linear length and because of the mismatches it is quite possible for the number of defects that participate in the current between electrodes to be considerably less than for a single crystal. Thus, if only 10% of the defects are effective in conduction, the noise would be higher by a factor of 10, about what is seen in Fig. 8. Of course, other causes such as grain-grain contacts and hygroscopic effects can also enhance the noise level, which may account for the wide variability found in Na- β'' -alumina ceramic specimens. Therefore, attempts to describe quantitatively diffusion noise in ceramics seem fruitless at present.

The $f^{-3/2}$ spectral shape characteristic of diffusion noise holds only above a characteristic turnover frequency given by $2\pi f_0 = 2D/l^2$, where l is the embedded area smallest dimension. For Na(1) and a 0.1-cm embedded sample length, the result is $f_0 = 4.8 \times 10^{-5}$ Hz, well below the experimental frequency range in Figs. 5-7. It is also possible to derive an experimental value for $2D/l^2$ by observing the time decay of the noise from a nonspatially homogeneous distribution of the mobile ions as the distribution returns to a uniform condition. The result,⁶ for a 0.8-cm long Na- β'' -alumina sample is 9×10^{-7} Hz,

which for a 0.1 cm sample becomes $f_0 = (0.8/0.1)^2 \times 9 \times 10^{-7} = 5.7 \times 10^{-5}$ Hz.

IV. CONCLUSIONS

This theory of two-dimensional diffusion noise is based closely on the observed crystallographic data and the results of diffuse x-ray and neutron scattering. The superlattice organization indicates that three "species" play a role in the ambipolar correlated motion: anti-BR site vacancies, BR cations, and anti-BR cations. The noise predicted by the theory resulting from this correlated motion in one plane gives the correct magnitude, as observed by experiment. The coherence lengths and coherence energy for antiferroelectric ordering within a plane obtained from the data are in good agreement with the literature. Furthermore, plasma-Coulomb interactions within the plane are completely screened and do not result in enhanced noise magnitude.

The noise from adjacent planes perpendicular to the c axis is completely correlated because of electrostatic induction coupling via the spinel blocks. This is concor-

dant with the observation that the two-dimensional structure patterns of platelets are not washed out by randomness along the c axis.

The reasons for the lack of agreement between theory and experiment in the case of Ag- β'' -alumina require further exploration. Also, it would be desirable to examine the applicability of the model to other mobile ion species, such as K- and Ca- β'' -alumina.

ACKNOWLEDGMENTS

This work was supported in part by the Office of Naval Research, and C. M. Van Vliet also acknowledges support from NSERC, Ottawa, under Grant No. A9522 and she thanks le Fonds FCAR, Québec, for supporting this research. J. J. Brophy expresses his appreciation to Chu Kun Kuo, Steven W. Smith, and Xiaoyi Wang, who carried out many of the experimental measurements. We also acknowledge discussions in the earlier stages of this work with Professor G. Forgacs of Clarkson University, N.Y., and Professor L. B. Kiss of Jate University, Hungary.

*Deceased.

- ¹J. B. Bates, J.-C. Wang, and N. J. Dudney, *Phys. Today* **63**(2), 46 (1982).
- ²J. J. Brophy and S. W. Smith, *J. Appl. Phys.* **58**, 351 (1985); *Noise in Physical Systems and 1/f Noise*, edited by A. D'Amico and P. Mazzetti (Elsevier, New York, 1986), p. 243.
- ³C. K. Kuo and J. J. Brophy, *J. Appl. Phys.* **65**, 3484 (1989).
- ⁴J. J. Brophy, *J. Appl. Phys.* **61**, 581 (1987).
- ⁵J. J. Brophy and J. J. Carroll, in *Ninth International Conference of Noise in Physical Systems*, Montreal, edited by C. M. Van Vliet (World Scientific, Singapore, 1987), p. 307.
- ⁶C. K. Kuo and J. J. Brophy, *Solid State Ion.* **25**, 193 (1987).
- ⁷C. K. Kuo and J. J. Brophy, *Solid State Ion.* **37**, 37 (1989); *J. Appl. Phys.* **68**, 4617 (1990).
- ⁸J. P. Scofield and W. W. Webb, *Phys. Rev. Lett.* **54**, 353 (1985).
- ⁹M. Lax and P. Mengert, *J. Phys. Chem. Solids* **14**, 248 (1960).
- ¹⁰J. L. Briant and G. C. Farrington, *J. Solid State Chem.* **33**, 385 (1980); R. SeEVERS, J. Denuzzio, and G. C. Farrington, *ibid.* **50**, 146 (1983).
- ¹¹J. P. Boilot, G. Collin, Ph. Colomban, and R. Comes, *Phys. Rev. B* **22**, 5912 (1980).
- ¹²G. Collin, J. P. Boilot, Ph. Colomban, and R. Comes, *Phys. Rev. B* **34**, 5838 (1986).
- ¹³G. Collin, J. P. Boilot, and R. Comes, *Phys. Rev. B* **34**, 5850 (1986).
- ¹⁴K. M. Van Vliet and J. R. Fassett, in *Fluctuation Phenomena in Solids*, edited by R. E. Burgess (Academic, New York, 1965), pp. 267-354.

- ¹⁵H. Mehta, Ph.D. thesis, University of Florida, 1981.
- ¹⁶K. M. Van Vliet and E. R. Chenette, *Physica* **31**, 985 (1965).
- ¹⁷R. E. Burgess, *Proc. Phys. Soc. London B* **66**, 334 (1953).
- ¹⁸R. Voss and J. Clarke, *Phys. Rev. B* **13**, 556 (1976).
- ¹⁹J. M. Richardson, *Bell Syst. Tech. J.* **29**, 117 (1950).
- ²⁰K. M. Van Vliet and H. Mehta, *Phys. Status Solidi (b)* **106**, 11 (1981).
- ²¹*Handbook of Mathematical Functions*, Natl. Bur. Stand. Appl. Math. Ser. No. 55, edited by M. Abramowitz and I. A. Stegun (U.S. GPO, Washington, D.C., 1964), Chap. 9.
- ²²I. S. Gradshteyn and I. M. Ryzhik, *Table of Integrals, Series and Products* (Academic, New York, 1980); see Eq. (3.241).
- ²³P. Debye and G. Hückel, *Phys. Z.* **24**, 305 (1923).
- ²⁴L. D. Landau and E. M. Lifshitz, *Statistical Physics* (Addison-Wesley, Reading, MA, 1958), p. 234ff.
- ²⁵K. M. Van Vliet, *J. Math. Phys.* **12**, 1981 (1971).
- ²⁶K. M. Van Vliet, *J. Math. Phys.* **12**, 1998 (1971).
- ²⁷G. Forgacs and L. B. Kiss (private communication).
- ²⁸M. C. Wang and G. E. Uhlenbeck, *Rev. Mod. Phys.* **17**, 323 (1945).
- ²⁹R. E. Burgess, *Physica* **20**, 1007 (1954).
- ³⁰Tahir-Keli and El-Meshad, *Phys. Rev. B* **32**, 6166 (1985).
- ³¹M. Abraham and R. Becker, *The Classical Theory of Electricity and Magnetism*, 2nd ed. (Hafner, New York, 1955), p. 65ff.
- ³²N. F. Mott and R. W. Gurney, *Electronic Processes in Ionic Crystals* (Oxford University, New York, 1940), Chap. II. (reprinted by Dover, New York, 1964).